

# Analysis of the non-linear behavior of micro-perforated plates using lattice Boltzmann method

**F. Chevillotte, P. Marchner, M. Martinez, R. Roncen, F. Simon**

fabien.chevillotte@matelys.com

SAPEM 2017, Le Mans

6-8 December 2017

**ONERA**

THE FRENCH AEROSPACE LAB



# Introduction

- The **linear acoustic behavior** of micro-perforated plates is **well understood**.
- The **non-linear behavior** under high sound pressure level (or submitted to a flow) has been studied but the models are **still limited**.
- The idea of this work is to analyse this non linear behavior at the **microscopic scale** using the **lattice Boltzmann method (LBM)** to improve analytical models.

# Introduction

- The **linear acoustic behavior** of micro-perforated plates is **well understood**.
- The **non-linear behavior** under high sound pressure level (or submitted to a flow) has been studied but the models are **still limited**.
- The idea of this work is to analyse this non linear behavior at the **microscopic scale** using the **lattice Boltzmann method (LBM)** to improve analytical models.

# Introduction

- The **linear acoustic behavior** of micro-perforated plates is **well understood**.
- The **non-linear behavior** under high sound pressure level (or submitted to a flow) has been studied but the models are **still limited**.
- The idea of this work is to analyse this non linear behavior at the **microscopic scale** using the **lattice Boltzmann method** (LBM) to improve analytical models.

# Modeling the linear behavior of micro-perforated plates

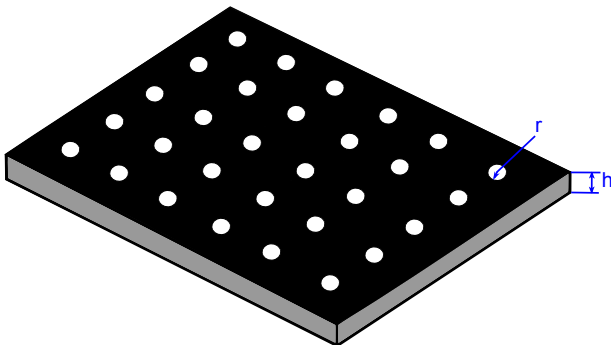
- Numerous analytical models can be found in the literature for modeling the linear behavior of micro-perforated plates :
  - **Ingard**, U. "On the theory and design of acoustic resonators." J. Acoust. Soc. Am., 25(6) :1037–1061, **1953**.
  - **Beranek**, L.L. and Ver, I.L. *Noise and Vibration Control Engineering*. Wiley, New York, **1992**.
  - **Maa**, D.-Y. "Potential of microperforated panel absorber." J. Acoust. Soc. Am., 104(5) :2861–2866, **1998**.
  - **Atalla** N, Sgard F. "Modeling of perforated plates and screens using rigid frame porous models", J. Sound Vib. 303 **2007**.
  - **Guo**, Y., Allam, Y., and Abom, M. "Micro-perforated plates for vehicle applications." In Proceedings Internoise 2008, Shanghai, China, **2008**.
  - **Bolton**, J.S. and Kim N., "Use of cfd to calculate the dynamic resistive end correction for microperforated materials." Acoustics Australia, 38 (3) :134 –144, **2010**.
  - ...

# Modeling the linear behavior of micro-perforated plates

- Numerous analytical models can be found in the literature for modeling the linear behavior of micro-perforated plates :
  - **Ingard**, U. "On the theory and design of acoustic resonators." J. Acoust. Soc. Am., 25(6) :1037–1061, **1953**.
  - **Beranek**, L.L. and Ver, I.L. *Noise and Vibration Control Engineering*. Wiley, New York, **1992**.
  - **Maa**, D.-Y. "Potential of microperforated panel absorber." J. Acoust. Soc. Am., 104(5) :2861–2866, **1998**.
  - **Atalla** N, Sgard F. "Modeling of perforated plates and screens using rigid frame porous models", J. Sound Vib. 303 **2007**.
  - **Guo**, Y., Allam, Y., and Abom, M. "Micro-perforated plates for vehicle applications." In Proceedings Internoise 2008, Shanghai, China, **2008**.
  - **Bolton**, J.S. and Kim N., "Use of cfd to calculate the dynamic resistive end correction for microperforated materials." Acoustics Australia, 38 (3) :134 –144, **2010**.
  - ...

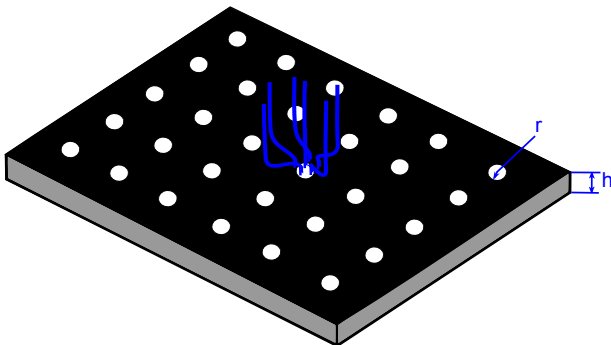
# Modeling the linear behavior of micro-perforated plates

- These models are based on the **same parameters** :  
 $r$  : perforation radius,  $\phi$  : perforation rate,  $h$  : plate thickness
- and generally differ in the way to take into account the **flow distortion** (resistance and reactance corrections)



# Modeling the linear behavior of micro-perforated plates

- These models are based on the **same parameters** :  
 $r$  : perforation radius,  $\phi$  : perforation rate,  $h$  : plate thickness
- and generally differ in the way to take into account the **flow distortion** (resistance and reactance corrections)





## Example of impedance models

- Maa's model (1998) :

$$\tilde{Z}_s = \frac{32\eta h}{\phi d^2} \left( \sqrt{1 + \frac{k^2}{32}} + \frac{\sqrt{2}}{32} k \frac{d}{h} \right) + j\omega \frac{\rho_0 h}{\phi} \left[ \left( 1 + \frac{1}{\sqrt{9 + \frac{k^2}{2}}} \right) + 0.85 \frac{d}{h} \right] + Z_B$$

$$d = 2r, R_s = \frac{1}{2} \sqrt{2\eta\omega\rho_0} \text{ and } k = \frac{2r}{\sqrt{2\eta}} R_s, Z_B : \text{backing impedance}$$

- Guo's model (2008) :

$$\tilde{Z}_s = \frac{j\rho_0\omega h}{\phi} \left[ 1 - \frac{2}{k\sqrt{-j}} \frac{J_1(k\sqrt{-j})}{J_0(k\sqrt{-j})} \right]^{-1} + \frac{\alpha 2R_s}{\phi} + j\omega\rho_0 \frac{\delta}{\phi} + Z_B \quad (1)$$

## Example of impedance models

- Maa's model (1998) :

$$\tilde{Z}_s = \frac{32\eta h}{\phi d^2} \left( \sqrt{1 + \frac{k^2}{32}} + \frac{\sqrt{2}}{32} k \frac{d}{h} \right) + j\omega \frac{\rho_0 h}{\phi} \left[ \left( 1 + \frac{1}{\sqrt{9 + \frac{k^2}{2}}} \right) + 0.85 \frac{d}{h} \right] + Z_B$$

$$d = 2r, R_s = \frac{1}{2} \sqrt{2\eta\omega\rho_0} \text{ and } k = \frac{2r}{\sqrt{2\eta}} R_s, Z_B : \text{backing impedance}$$

- Guo's model (2008) :

$$\tilde{Z}_s = \frac{j\rho_0\omega h}{\phi} \left[ 1 - \frac{2}{k\sqrt{-j}} \frac{J_1(k\sqrt{-j})}{J_0(k\sqrt{-j})} \right]^{-1} + \frac{\alpha 2R_s}{\phi} + j\omega\rho_0 \frac{\delta}{\phi} + Z_B \quad (1)$$

# Modeling a perforated plate as a porous medium

- A **perforated plate** may be viewed as a **porous material**.
- **Macroscopic parameters using the 5-parameter JCA model :**

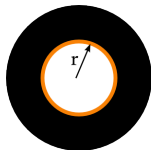
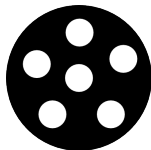
$\phi$  : perforation rate

$$\Lambda = \Lambda' = r$$

$$\sigma = \frac{8\eta}{\phi r^2}$$

$$\alpha_\infty = 1 + \frac{n\epsilon}{h}$$

Atalla N, Sgard F. "Modeling of perforated plates and screens using rigid frame porous models", J. Sound Vib. 303 (2007).



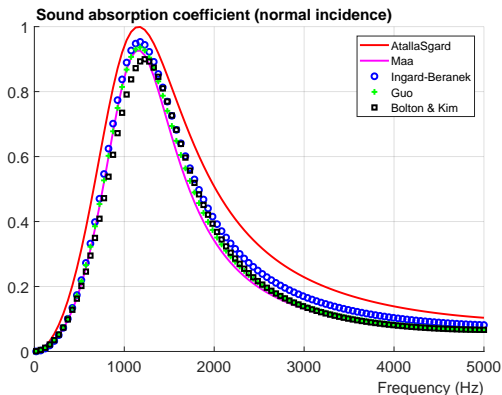
$h$  : Thickness of the plate

$\epsilon$  : Length correction

$n$  : Factor depending on the nature of upstream and downstream materials

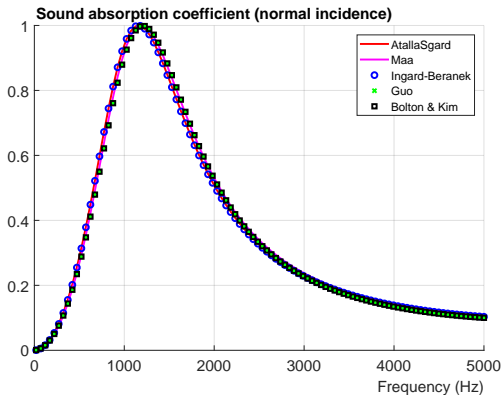
# Modeling the linear behavior of micro-perforated plates

- Comparison of linear models using **original corrections**.



$$\phi = 0.025, h = 1 \text{ mm}, d = 1 \text{ mm}, L_c = 20 \text{ mm}, \text{glasswool } \sigma \approx 10\,000 \text{ N.s.m}^{-4}$$

- Comparison of linear models using the **same correction**.



$\epsilon$  can be computed for any shape of perforation in the full range of porosity [0-1].

Ingard, U. "On the theory and design of acoustic resonators." J. Acoust. Soc. Am., 1953.

Jaouen, L., Chevillotte, F. "Length correction of 2D discontinuities at large wavelengths and for linear acoustics." submitted to Acta Acustica 2017

# Non-linear regime behavior

- Melling has studied this non-linear effect for perforated plates submitted to a high sound pressure level :

$$R_t = R_{lin}(L_p) + \frac{\rho_0}{2} \frac{8}{3\pi} \frac{1}{C_d^2} \frac{1 - \phi^2}{\phi^2} U$$

with  $R_t = \sigma_t L_p$  the airflow resistance,

- The **non-linear term** is proportional to the **velocity level**  $U$  and depends on the **open porosity**  $\phi$  and a **discharge coefficient**  $C_d$ .
- $C_d$  is generally obtained from experiments.

Melling, T.H., "The acoustic impedance of perforates at medium and high sound levels," J. Sound. Vib., Vol. 29(1), 1973, pp. 1-65.

# Non-linear regime behavior

- Melling has studied this non-linear effect for perforated plates submitted to a high sound pressure level :

$$R_t = R_{lin}(L_p) + \frac{\rho_0}{2} \frac{8}{3\pi} \frac{1}{C_d^2} \frac{1 - \phi^2}{\phi^2} U$$

with  $R_t = \sigma_t L_p$  the airflow resistance,

- The **non-linear term** is proportional to the **velocity level**  $U$  and depends on the **open porosity**  $\phi$  and a **discharge coefficient**  $C_d$ .
- $C_d$  is generally obtained from experiments.

Melling, T.H., "The acoustic impedance of perforates at medium and high sound levels," J. Sound. Vib., Vol. 29(1), 1973, pp. 1-65.

## Non-linear regime behavior

- Melling has studied this non-linear effect for perforated plates submitted to a high sound pressure level :

$$R_t = R_{lin}(L_p) + \frac{\rho_0}{2} \frac{8}{3\pi} \frac{1}{C_d^2} \frac{1 - \phi^2}{\phi^2} U$$

with  $R_t = \sigma_t L_p$  the airflow resistance,

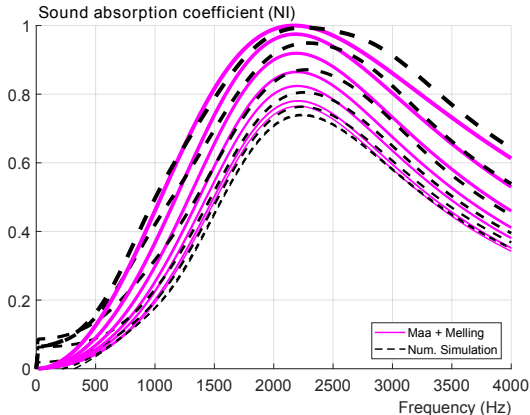
- The **non-linear term** is proportional to the **velocity level**  $U$  and depends on the **open porosity**  $\phi$  and a **discharge coefficient**  $C_d$ .
- $C_d$  is generally obtained from experiments.

Melling, T.H., "The acoustic impedance of perforates at medium and high sound levels," J. Sound. Vib., Vol. 29(1), 1973, pp. 1-65.



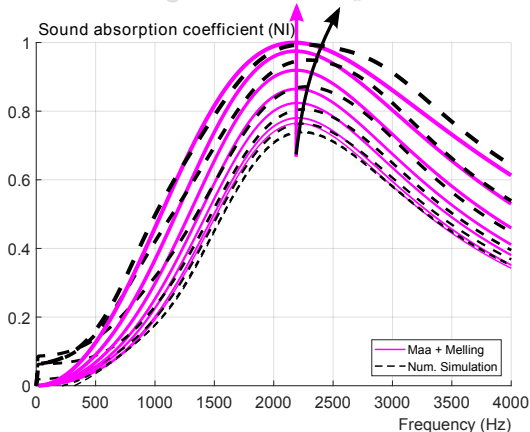
# Non-linear regime behavior

- Melling's model **does** predict the shift in amplitude with SPL,
- but **does not** predict the shift in frequency with SPL,
- and requires a **discharge coefficient**  $C_d$ .



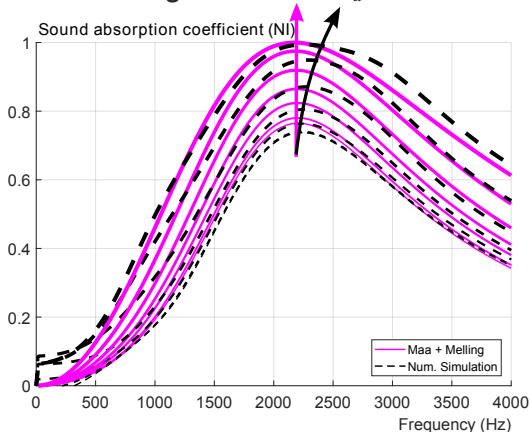
## Non-linear regime behavior

- Melling's model **does** predict the shift in amplitude with SPL,
- but **does not** predict the shift in frequency with SPL,
- and requires a **discharge coefficient**  $C_d$ .

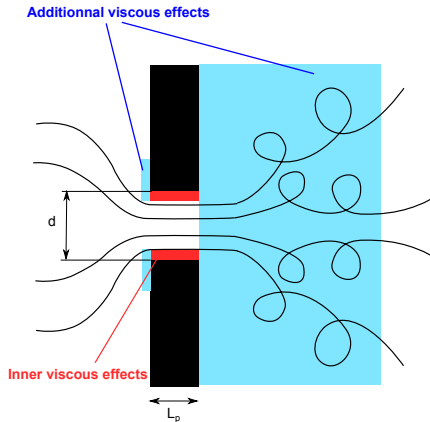


# Non-linear regime behavior

- Melling's model **does** predict the shift in amplitude with SPL,
- but **does not** predict the shift in frequency with SPL,
- and requires a **discharge coefficient**  $C_d$ .

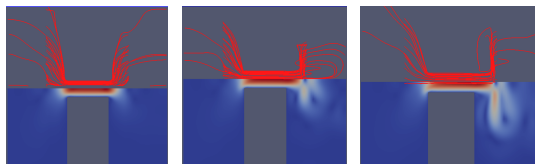
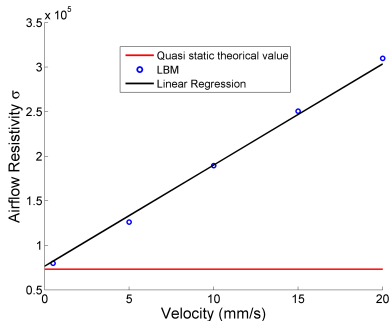


## Analysis at the microscopic level



$$R_t(\phi, L_p, U, d) = R_p(\phi, L_p, U, d) + R_r(\phi, U)$$

# Modeling from the microstructure

a)  $U = 0.5 \text{ mm.s}^{-1}$ b)  $U = 5 \text{ mm.s}^{-1}$ c)  $U = 10 \text{ mm.s}^{-1}$ 

## Analysis at the microscopic level

- The total resistance is the sum of the **inner** viscous effects  $R_p$  and the **additional viscous effects**  $R_r$  :

$$R_t(\phi, L_p, U, d) = R_p(\phi, L_p, U, d) + R_r(\phi, U)$$

- The inner resistance  $R_p$  is proportional to the airflow resistivity  $\sigma_p$  :

$$R_t(\phi, L_p, U, d) = \sigma_p(\phi, U, d) L_p + R_r(\phi, U)$$

- Both the inner and the additional viscous effects may have a non linear behavior :

$$R_t(\phi, L_p, U, d) = (\sigma_{p0} + \sigma_{pi}|U|) L_p + R_{r0} + R_{ri}|U|$$

## Analysis at the microscopic level

- The total resistance is the sum of the **inner** viscous effects  $R_p$  and the **additional viscous effects**  $R_r$  :

$$R_t(\phi, L_p, U, d) = R_p(\phi, L_p, U, d) + R_r(\phi, U)$$

- The inner resistance  $R_p$  is proportional to the airflow resistivity  $\sigma_p$  :

$$R_t(\phi, L_p, U, d) = \sigma_p(\phi, U, d) L_p + R_r(\phi, U)$$

- Both the inner and the additional viscous effects may have a non linear behavior :

$$R_t(\phi, L_p, U, d) = (\sigma_{p0} + \sigma_{pi}|U|) L_p + R_{r0} + R_{ri}|U|$$

## Analysis at the microscopic level

- The total resistance is the sum of the **inner** viscous effects  $R_p$  and the **additional viscous effects**  $R_r$  :

$$R_t(\phi, L_p, U, d) = R_p(\phi, L_p, U, d) + R_r(\phi, U)$$

- The inner resistance  $R_p$  is proportional to the airflow resistivity  $\sigma_p$  :

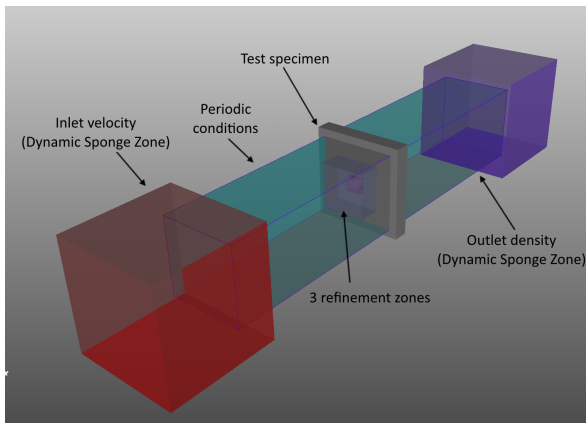
$$R_t(\phi, L_p, U, d) = \sigma_p(\phi, U, d) L_p + R_r(\phi, U)$$

- Both the inner and the additional viscous effects may have a non linear behavior :

$$R_t(\phi, L_p, U, d) = (\sigma_{p0} + \sigma_{pi}|U|) L_p + R_{r0} + R_{ri}|U|$$

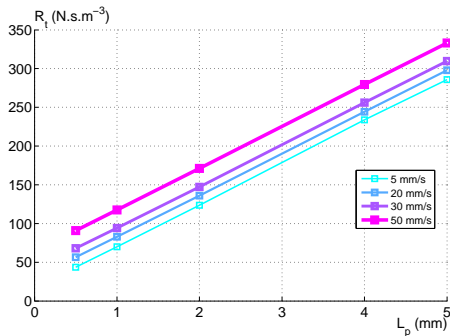


- A parametric study has been carried out in order to determine these coefficients.
  - Perforation thickness  $L_p \in [0.5 - 5 \text{ mm}]$
  - Perforation diameter  $d \in [0.5 - 4 \text{ mm}]$
  - Perforation rate  $\phi \in [0.0314 - 0.503]$ .



## Airflow resistance determination

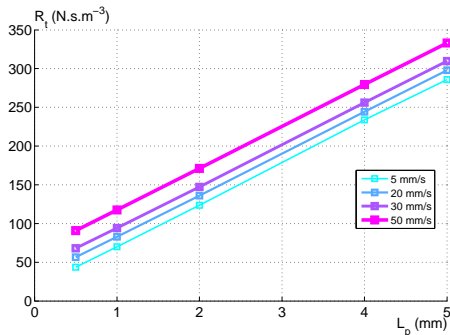
- Airflow resistance as a function of the perforation thickness for 4 upstream velocity levels :



- The ordinates correspond to the added resistance  $R_r$
- The slopes give the airflow resistivity  $\sigma_p$

## Airflow resistance determination

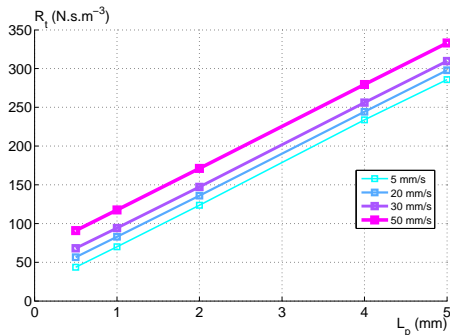
- Airflow resistance as a function of the perforation thickness for 4 upstream velocity levels :



- The ordinates correspond to the added resistance  $R_r$
- The slopes give the airflow resistivity  $\sigma_p$

## Airflow resistance determination

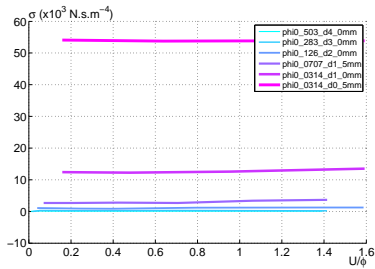
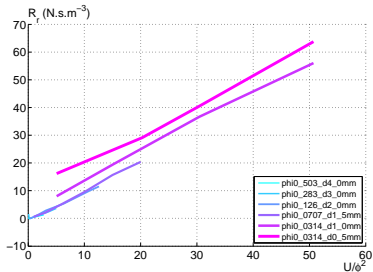
- Airflow resistance as a function of the perforation thickness for 4 upstream velocity levels :



- The ordinates correspond to the added resistance  $R_r$
- The slopes give the airflow resistivity  $\sigma_p$

# Airflow resistance determination

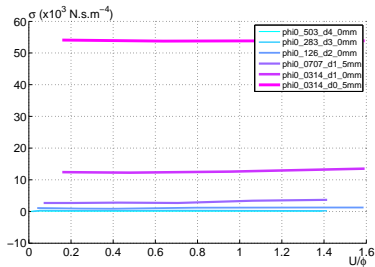
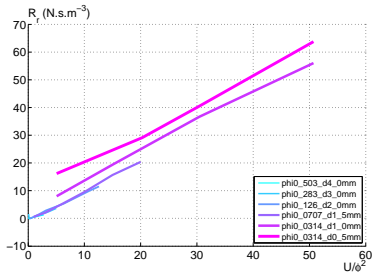
- Extraction of  $R_r$  and  $\sigma_p$  :



- The inner effects  $\sigma_p$  do not show a non-linear behavior for this range of upstream velocity.
- The **non-linear behavior** strongly depends on the **downstream flow distortion** and seems proportional to  $U/\phi^2$  (as Melling's non-linear term).
- Numerical methodology to determine the **discharge coefficient  $C_d$** .

# Airflow resistance determination

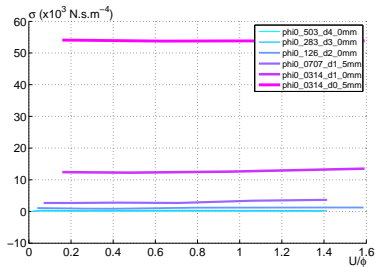
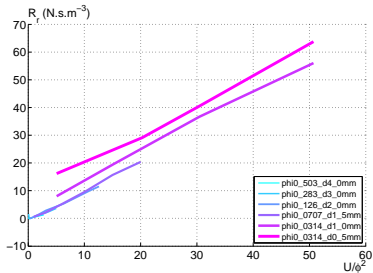
- Extraction of  $R_r$  and  $\sigma_p$  :



- The inner effects  $\sigma_p$  do not show a non-linear behavior for this range of upstream velocity.
- The **non-linear behavior** strongly depends on the **downstream flow distortion** and seems proportional to  $U/\phi^2$  (as Melling's non-linear term).
- Numerical methodology** to determine the **discharge coefficient**  $C_d$ .

# Airflow resistance determination

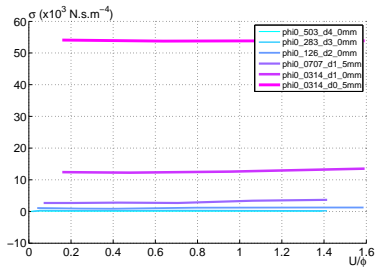
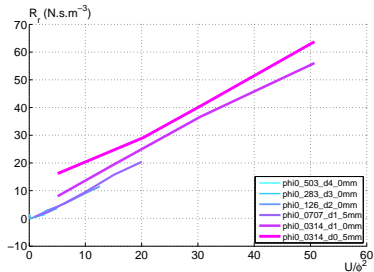
- Extraction of  $R_r$  and  $\sigma_p$  :



- The inner effects  $\sigma_p$  do not show a non-linear behavior for this range of upstream velocity.
- The **non-linear behavior** strongly depends on the **downstream flow distorsion** and seems proportional to  $U/\phi^2$  (as Melling's non-linear term).
- Numerical methodology to determine the **discharge coefficient**  $C_d$ .

# Airflow resistance determination

- Extraction of  $R_r$  and  $\sigma_p$  :



- The inner effects  $\sigma_p$  do not show a non-linear behavior for this range of upstream velocity.
- The **non-linear behavior** strongly depends on the **downstream flow distorsion** and seems proportional to  $U/\phi^2$  (as Melling's non-linear term).
- Numerical methodology** to determine the **discharge coefficient**  $C_d$ .



# Proposed non-linear model

- **Macroscopic parameters using the 5-parameter JCA model :**

- From geometrical parameters :

$\phi$  : perforation rate

$\Lambda = \Lambda' = r$  ( $\Lambda$  is computed for a perfect non-viscous fluid)

- Correction of low frequency viscous effect :

$$\sigma = \frac{8\eta}{\phi r^2} + \frac{R_r}{L}$$

- Inertial effect (length correction) :

$$\alpha_\infty = 1 + \frac{n\epsilon}{L}$$

$\epsilon$  can be computed for any shape of perforation in the full range of porosity [0-1].

- The 5-parameter JCA model enables to independently control the low and high frequency asymptotic behaviors.

# Proposed non-linear model

- **Macroscopic parameters using the 5-parameter JCA model :**

- From geometrical parameters :

$\phi$  : perforation rate

$$\Lambda = \Lambda' = r \quad (\Lambda \text{ is computed for a perfect non-viscous fluid})$$

- Correction of low frequency viscous effect :

$$\sigma = \frac{8\eta}{\phi r^2} + \frac{R_f}{L}$$

- Inertial effect (length correction) :

$$\alpha_\infty = 1 + \frac{n\epsilon}{L}$$

$\epsilon$  can be computed for any shape of perforation in the full range of porosity [0-1].

- The 5-parameter JCA model enables to **independently control the low and high frequency asymptotic behaviors.**

# Proposed non-linear model

- **Macroscopic parameters using the 5-parameter JCA model :**

- From geometrical parameters :

$\phi$  : perforation rate

$\Lambda = \Lambda' = r$  ( $\Lambda$  is computed for a perfect non-viscous fluid)

- Correction of low frequency viscous effect :

$$\sigma = \frac{8\eta}{\phi r^2} + \frac{R_r}{L}$$

- Inertial effect (length correction) :

$$\alpha_\infty = 1 + \frac{n\epsilon}{L}$$

$\epsilon$  can be computed for any shape of perforation in the full range of porosity [0-1].

- The 5-parameter JCA model enables to **independently control the low and high frequency asymptotic behaviors.**

# Proposed non-linear model

- **Macroscopic parameters using the 5-parameter JCA model :**

- From geometrical parameters :

$\phi$  : perforation rate

$\Lambda = \Lambda' = r$  ( $\Lambda$  is computed for a perfect non-viscous fluid)

- Correction of low frequency viscous effect :

$$\sigma = \frac{8\eta}{\phi r^2} + \frac{R_r}{L}$$

- Inertial effect (length correction) :

$$\alpha_\infty = 1 + \frac{n\epsilon}{L}$$

$\epsilon$  can be computed for any shape of perforation in the full range of porosity [0-1].

- The 5-parameter JCA model enables to **independently control the low and high frequency asymptotic behaviors.**

# Proposed non-linear model

- **Macroscopic parameters using the 5-parameter JCA model :**

- From geometrical parameters :

$\phi$  : perforation rate

$$\Lambda = \Lambda' = r \quad (\Lambda \text{ is computed for a perfect non-viscous fluid})$$

- Correction of low frequency viscous effect :

$$\sigma = \frac{8\eta}{\phi r^2} + \frac{R_r}{L}$$

- Inertial effect (length correction) :

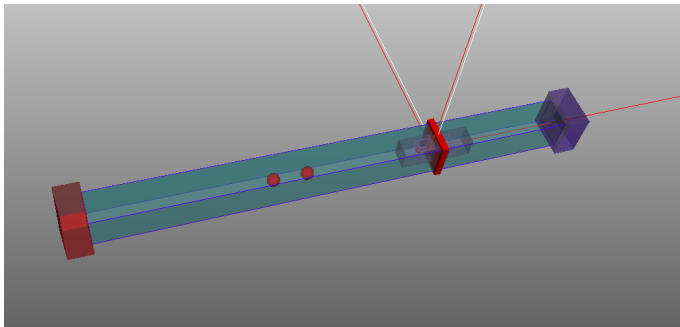
$$\alpha_\infty = 1 + \frac{n\epsilon}{L}$$

$\epsilon$  can be computed for any shape of perforation in the full range of porosity [0-1].

- The 5-parameter JCA model enables to **independently control the low and high frequency asymptotic behaviors.**

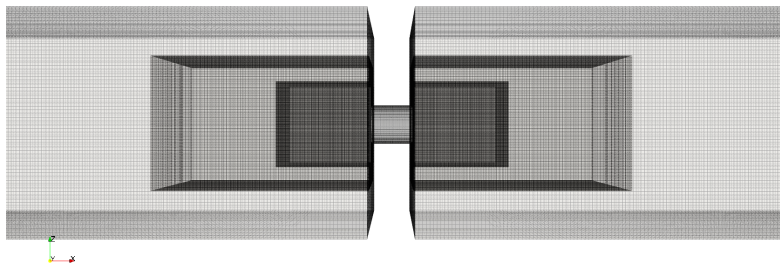


# Dynamic simulation under high SPL using LBM



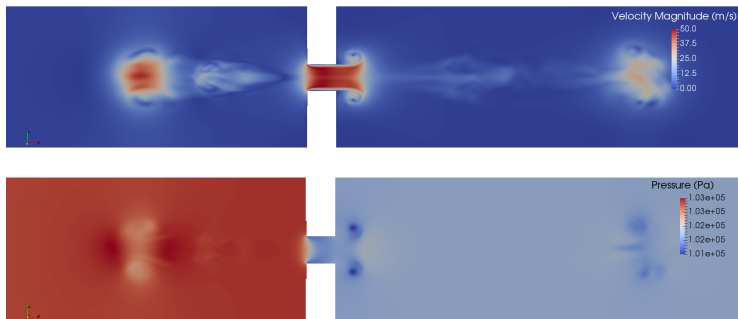
- Perforated plate submitted to a dynamic excitation,
- Considered excitations :
  - Pulse : wide frequency band without control of the overall level,
  - Sine : control of the level for a single frequency,
  - Chirp : wide frequency band with control of the overall level.

# Mesh around aperture





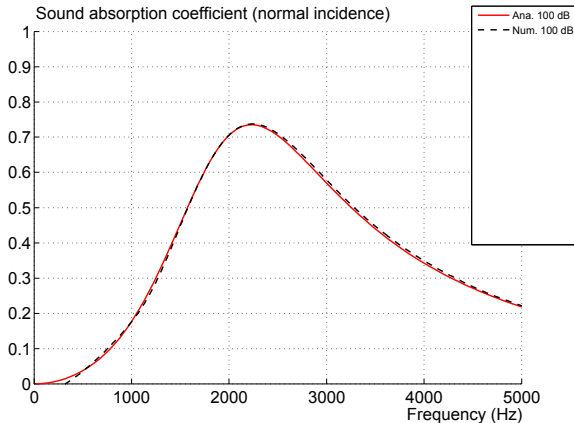
# Dynamic simulation under high SPL using LBM



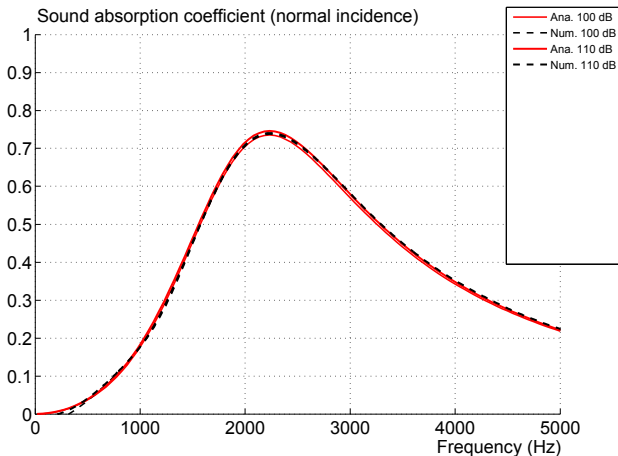
Simulation with a sine excitation at 151 dB.

# Effect of the sound pressure level on the sound absorption coefficient

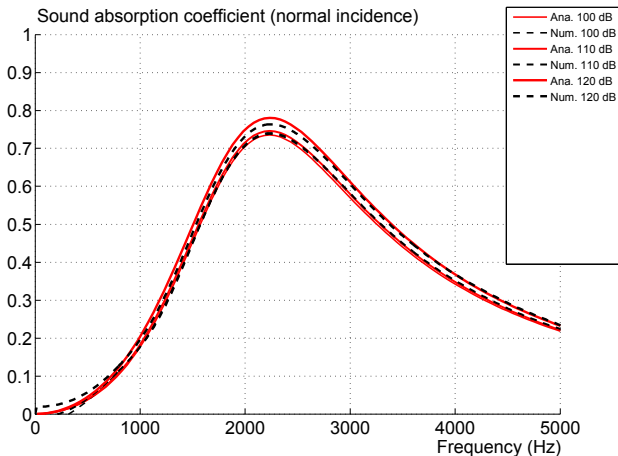
$$\phi = 0.05, d = 0.3 \text{ mm}, h = 0.8 \text{ mm}$$



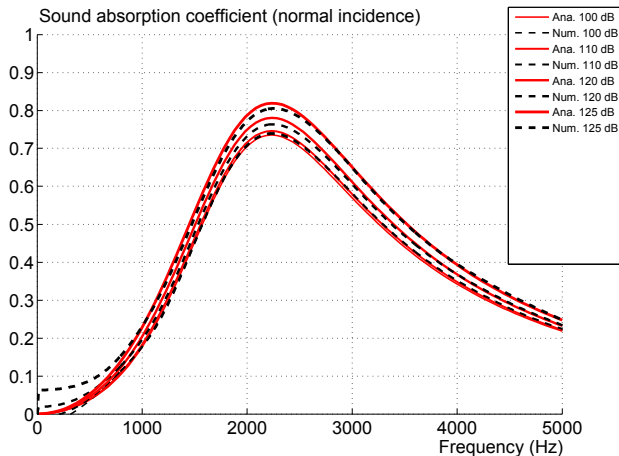
# Effect of the sound pressure level on the sound absorption coefficient



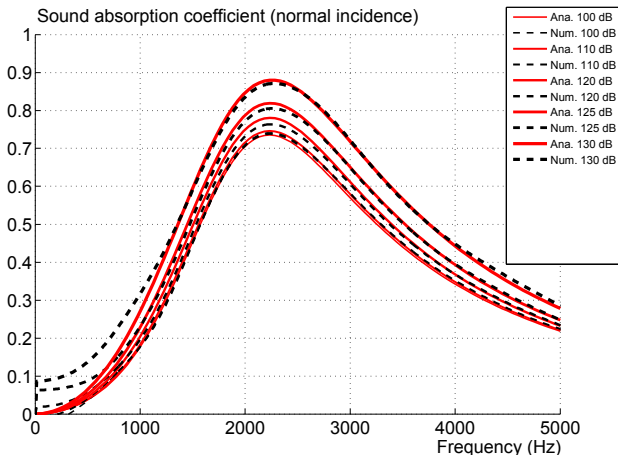
# Effect of the sound pressure level on the sound absorption coefficient



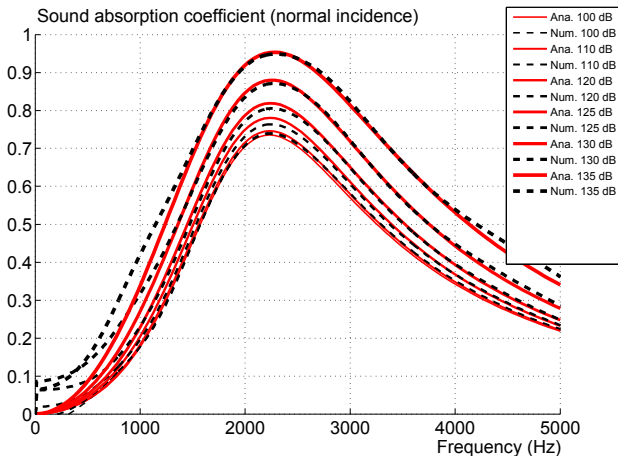
# Effect of the sound pressure level on the sound absorption coefficient



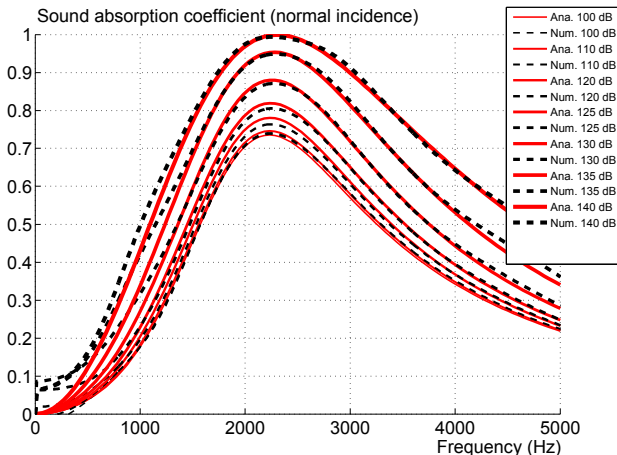
# Effect of the sound pressure level on the sound absorption coefficient



# Effect of the sound pressure level on the sound absorption coefficient

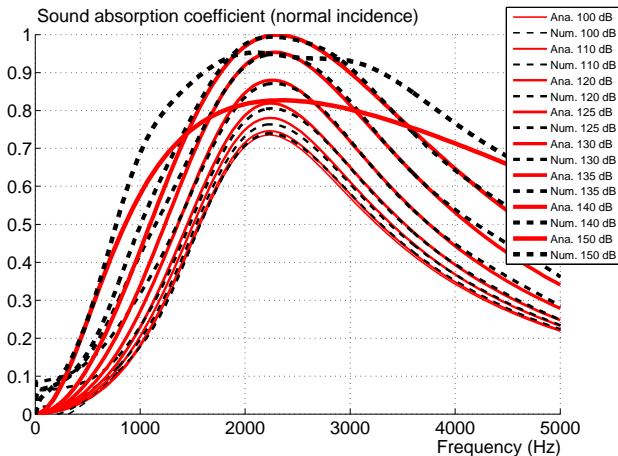


# Effect of the sound pressure level on the sound absorption coefficient

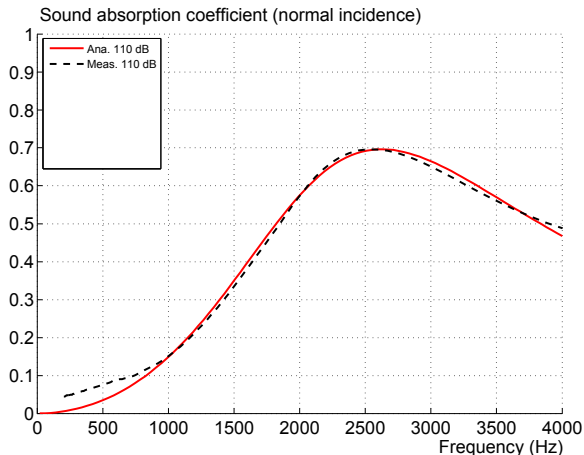


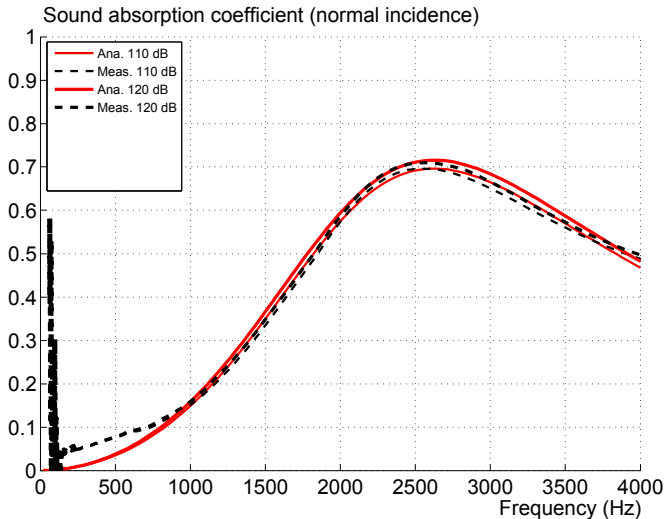


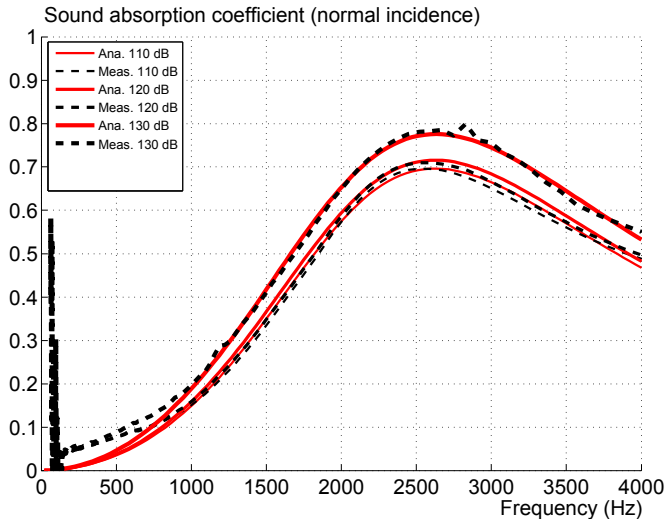
# Effect of the sound pressure level on the sound absorption coefficient

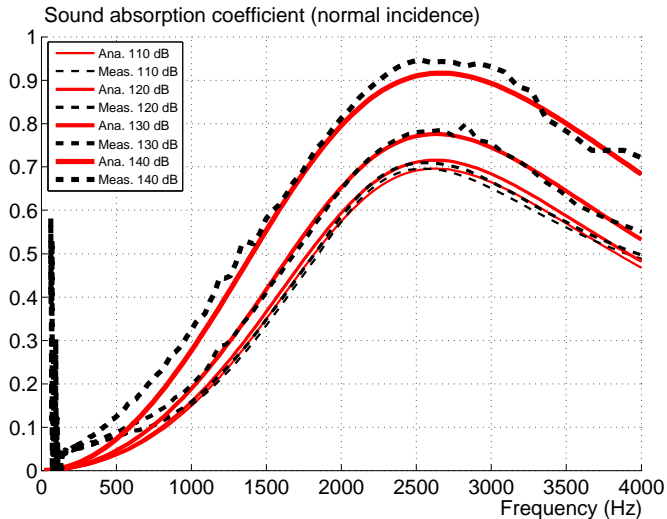


- Parameters have been estimated from the linear behavior :  
 $\phi = 0.075$ ,  $d = 0.25 \text{ mm}$ ,  $h = 0.8 \text{ mm}$ ,  $L_c = 20 \text{ mm}$  ;









# Conclusion

- The non-linear behavior of perforated plates has been studied thanks to LBM simulations.
- The non-linear resistance introduced by Melling seems to be confirmed.
- Airflow resistivity and discharge coefficient can be obtained by simulation at the microscopic level.
- The 5-parameter JCA model enables to independently control the low and high frequency asymptotic behaviors.
- The shifts in amplitude and frequency seem to be correctly predicted.
- Further configurations have to be studied.

# Conclusion

- The non-linear behavior of perforated plates has been studied thanks to LBM simulations.
- The non-linear resistance introduced by Melling seems to be confirmed.
- Airflow resistivity and discharge coefficient can be obtained by simulation at the microscopic level.
- The 5-parameter JCA model enables to independently control the low and high frequency asymptotic behaviors.
- The shifts in amplitude and frequency seem to be correctly predicted.
- Further configurations have to be studied.

# Conclusion

- The non-linear behavior of perforated plates has been studied thanks to LBM simulations.
- The non-linear resistance introduced by Melling seems to be confirmed.
- Airflow resistivity and discharge coefficient can be obtained by simulation at the microscopic level.
- The 5-parameter JCA model enables to independently control the low and high frequency asymptotic behaviors.
- The shifts in amplitude and frequency seem to be correctly predicted.
- Further configurations have to be studied.



# Conclusion

- The non-linear behavior of perforated plates has been studied thanks to LBM simulations.
- The non-linear resistance introduced by Melling seems to be confirmed.
- Airflow resistivity and discharge coefficient can be obtained by simulation at the microscopic level.
- The 5-parameter JCA model enables to independently control the low and high frequency asymptotic behaviors.
- The shifts in amplitude and frequency seem to be correctly predicted.
- Further configurations have to be studied.

# Conclusion

- The non-linear behavior of perforated plates has been studied thanks to LBM simulations.
- The non-linear resistance introduced by Melling seems to be confirmed.
- Airflow resistivity and discharge coefficient can be obtained by simulation at the microscopic level.
- The 5-parameter JCA model enables to independently control the low and high frequency asymptotic behaviors.
- The shifts in amplitude and frequency seem to be correctly predicted.
- Further configurations have to be studied.

# Conclusion

- The non-linear behavior of perforated plates has been studied thanks to LBM simulations.
- The non-linear resistance introduced by Melling seems to be confirmed.
- Airflow resistivity and discharge coefficient can be obtained by simulation at the microscopic level.
- The 5-parameter JCA model enables to independently control the low and high frequency asymptotic behaviors.
- The shifts in amplitude and frequency seem to be correctly predicted.
- Further configurations have to be studied.

## Conclusion

# Thank You For Your Attention !

